River Flow 2010 - Dittrich, Koll, Aberle & Geisenhainer (eds) - © 2010 Bundesanstalt für Wasserbau ISBN 978-3-939230-00-7

Contribution of Secondary Currents to Momentum Fluxes in Natural River Flows

Ch. Noß
Institute for Environmental Science, University of Koblenz-Landau, Landau, Germany

Th. Salzmann & I. Storchenegger
Institute for Environmental Engineering, University of Rostock, Rostock, Germany

A. Dittrich
Leichtweiß-Institut für Wasserbau, TU Braunschweig, Braunschweig, Germany

ABSTRACT: Totally 34 cross-sectional ADV measurements were carried out at five cross-sections of two small lowland river sections. One of the sections was returned to a near-natural condition. Abandoning river maintenance led to undulating bars at the second river section. Velocity distributions at these investigated sections indicated, that the stream characteristics did not agree with laws of the theorems of two-dimensional boundary layer and turbulence. Additional analysis of momentum fluxes were carried out and demonstrated the dominating contribution of secondary currents and the negligible contribution of Reynolds stresses to total momentum transport at these river sections.

Keywords: Nonuniform flow, Secondary currents, Shear stress, ADV, Field Site

1 INTRODUCTION

Knowledge about fluid motion and forces is necessary for planning and assessing near natural flows. However, the computation of the hydraulic conveyance, sediment transport and river bed stability of natural flows is – as far as possible – much more complicated in comparison to the computation of flows in technical constructed straight sections. Natural flows are mainly non-uniform. This non-uniformity is the result, but also the cause of heterogeneous river bed forms and irregularly distributed river bed roughness.

However, most of the models of open channel flows are based on approximations and cognitions concerning pipe flows. E.g. Prandtl's mixing length hypothesis for estimating turbulent covariance, hence the Reynolds shear stress and furthermore the law of the wall are suitable in open channel flows under the assumption of stationary uniform flow conditions without secondary currents. Because it is still impossible to describe the secondary currents in natural rivers (Sukhodolov et al. 2009), flow equations derived from the law of the wall are common approaches for non-uniform flows (Bravard & Petit 2009). Numerous studies focused on the flow and turbulence structures and on the shear stresses in natural flows or above morphological structures (Falcón & Kennedy 1983, Manga & Kirchner 2000, Carollo et al. 2002). As a result of these studies, the velocity distributions deviated from a logarithmical and the shear stress distributions deviated from a linear relationship to the boundary in vicinity to roughness elements (Stephan & Gutknecht 2002) and in the outer flow (Wang et al. 2001) as well as in the whole flow field, if the relative flow depth is low (Nikora et al. 2007). That means, that even a mild three-dimensionality of flows caused by secondary currents will produce false results of two-dimensional turbulence models (Bradshaw 1987).

Secondary currents, i.e. currents of perpendicular direction to the main flow, cause momentum fluxes, which equal local imbalances of forces. One can distinguish secondary currents of Prandtl's first kind or skew induced secondary currents caused by inertia driven forces, and secondary currents of Prandtl's second kind, i.e. turbulence induced secondary currents. Some cases of both secondary currents were already investigated in detail. Examples are the inertia induced secondary currents at curvatures (Boxhall et al. 2003), at groyne fields (Sukhodolov et al. 2002) or at confluences (Rhoads & Sukhodolov 2001) as well as turbulence induced secondary currents above roughness distributions (Nezu & Nakagawa 1993) or at composed cross-sections (Sanjou et al. 2006).

But little is known about the secondary currents and their contribution to the momentum fluxes in complex flow fields caused by patchy and mutual hydraulically interacting morphological structures. At small natural rivers, it is unlikely, that secondary currents are distinguishable into first and second kind. The scope of this study is to present velocity distributions, combined secondary currents of both types and momentum fluxes of natural flows from extensive field measurements at five cross-sections of two creeks. The non-uniform river bed and the dynamics of discharge and morphology are posing a challenge for collecting and processing the data. Therefore field sites and methods to filter and to align the velocity data will be shown in front of the results.

2 FIELD MEASUREMENTS AND DATA PROCESSING

Three-dimensional velocity distributions were measured at totally 34 dates at two small rivers, Hellbach and Nebel, in north-east Germany. These measurements were performed at different discharge rates. Fig. 1 shows the five investigated cross-sections. The Hellbach has been restored to a near-natural condition ten years ago. The shape of the Hellbach river bed was highly non-uniform and a broad range of morphologic structures, e.g. of woody debris or different grain sizes, was distributed irregularly. The river bed geometries, especially the cross-sectional geometries and the water levels were measured by an automatic level and by a tachymeter to estimate, e.g., the wetted perimeter, the cross-sectional area or the water level slope. Cross-section No.1 (Fig. 1) was situated at an approximately straight backwater section with a slightly widening behind a washed out root at the left bank side. Cross-section No.2 was situated at the apex of a strong curvature with a centerline radius of approximately four meter. Cross-section No.3 represented a straight section with a slightly higher slope of the riverbed than the two other cross-sections. The investigated Nebel-section was a straight constructed channel for drainage the riverine grassland. Undulating bars at this section were caused by deposition of sediments and organic material in dense reed-vegetations. At the cross-section No.4, the reed-bank was on the right-hand side. At the cross-section No.5, it was on the left-hand side. Three-dimensional velocity components were measured at a sampling frequency of 25 Hz by an acoustic Doppler velocimeter (ADV) device (Lohrmann et al. 1994, McLelland & Nicholas 2000). The ADV was mounted on a cable car like structure, spanned over the cross-section by three points. Two abutments at the top of the banks and a guide bar to the bottom fix the ADV probe and hence the sampling volumes in one measurement plane. This structure caused no disturbances at the natural developed cross-sectional shapes and its interaction with the stream was negligible. At each cross section the currents were measured at a series of points: small sampling volumes of approx. 0.25 cm³ were distributed along a series of vertical profiles located at various lateral positions along cross sectional width. Vertical displacements of 2 cm to 15 cm between the measurement points and lateral displacements of 0.50 m to 0.75 m between the verticals were chosen in respect to visually expected velocity gradients also observed in the on-line data. Therefore short displacements were chosen close to the river bed and at the boundaries of wakes, while large displacements were chosen, e.g. in dead zones. The total point densities were 25 m^{-2} at the Hellbach and 12 m^{-2} at the Nebel. Every ADV-point was sampled about 90 s to 120 s, which achieved the minimal record length ascertained by Lesht (1980) and Buffin-Bélanger & Roy (2005). Water surfaces

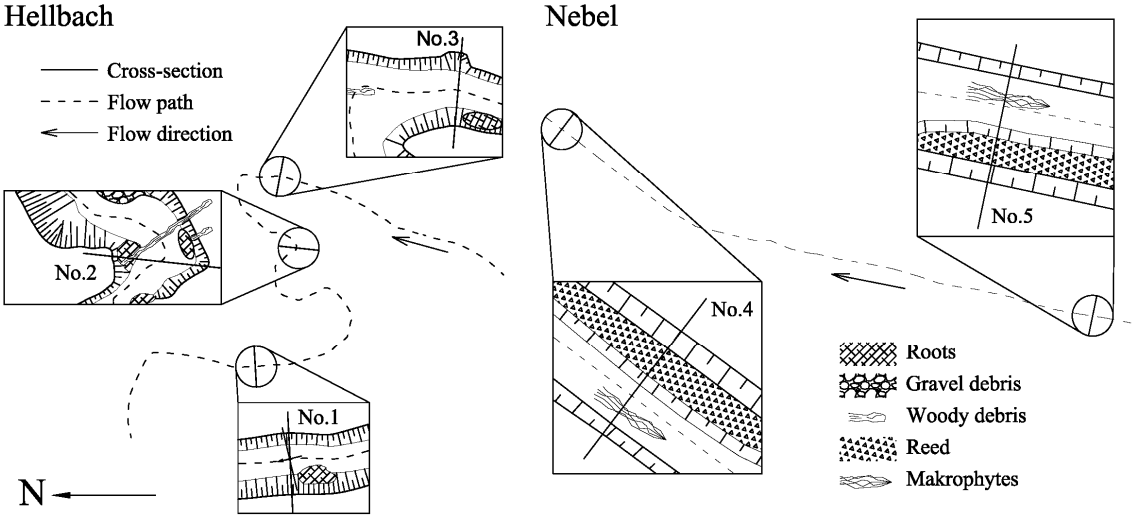

Figure 1. River reaches and cross-sections at Hellbach and Nebel

were measured at the beginning and at the end of each cross-sectional measurement to check stationary conditions during the collection of velocity data. Acquired data exhibit noise and outliers, so-called spikes and were filtered by the Phase-Space-Threshold method as described in detail by Goring & Nikora (2002). The original progression of spike-filtering was modified by (a) keeping the initial value, acceleration and skewness of the velocity and renewing the thresholds for spike-filtering on basis of the remaining velocities not detected as spikes until the iteration has finished, (b) an additional noise filter and (c) interpolating lags through a spline. Only small lags with less than 11 contiguous spikes in the series were filled up. Series with larger lags or totally more than 10 % spikes were removed to prevent analyzing artificial data.

Subsequent to the filtering, the raw velocity data must be realigned, because the raw velocity components were aligned in respect to East-North-Up or to the local coordinate system of the ADV-probe mounted on the cable car structure. It is unlikely, that the axes of these co-ordinate systems are identical with the longitudinal x-axis along the cross-sectional streamline, the lateral y-axis and vertical z-axis perpendicular to the streamline. Even at the same cross-section, the streamline has to be recalculated for every measurement due to the morphodynamic of the river bed and different discharge rates. We suggest transforming the velocity components on the assumption that the sum of all measured longitudinal velocity components in a cross-section should be maximized, while the sum of all lateral and the sum of all vertical velocity components should be zero, i.e. no in- and outflow occurs across the river bed and the water surface of the cross-section. This condition leads to the rotation angles

$$\alpha = \arctan\left(\frac{\langle v_m \rangle}{\langle u_m \rangle}\right) \tag{1}$$

around the measured vertical axis of the ADV-probes or Up-axis and

$$\beta = \arctan\left(\frac{\langle w_m \rangle}{\langle u_m \rangle \cdot \cos\alpha + \langle v_m \rangle \cdot \sin\alpha}\right) \tag{2}$$

around the new lateral y-axis, where u_m = longitudinal, v_m = lateral, w_m = vertical measured, but already filtered velocity components in the longitudinal, lateral and vertical direction of the ADV-probes and in east, north, up direction, respectively. The squared brackets denote spatial averaging, in this case across the cross-section. The transformation matrix

$$[T] = \begin{pmatrix} \cos\beta\cos\alpha & \cos\beta\sin\alpha & \sin\alpha \\ -\sin\alpha & \cos\alpha & 0 \\ -\sin\beta\cos\alpha & -\sin\beta\sin\alpha & \cos\alpha \end{pmatrix} \tag{3}$$

enables to realign the velocity components u in parallel, v lateral and w vertical to the streamline. Mean velocities are the flow velocity $\underline{u}$ and the secondary currents $\underline{v}$ and $\underline{w}$, where the overline denotes time-averaged and Reynolds-averaged, respectively.

3 ANALYSIS AND RESULTS

Tab.1 shows the observed ranges of hydrometric parameters at the investigated cross-sections. All flows were turbulent and subcritical.
Fig.2a-e shows examples of the flow velocities

Table 1. Range of hydrometric data at the investigated cross-sections

Cross-Section No.	Q [m³ s^{-1}]	A [m²]	r_{Hy} [m]	Re [×10^4]	Fr [1]	u^* [m s^{-1}]
Hellbach						
No.1	0.06 ... 1.56	0.98 ... 3.77	0.26 ... 0.65	5 ... 82	0.03 ... 0.14	0.04 ... 0.07
No.2	0.06 ... 1.56	1.46 ... 4.86	0.24 ... 0.62	3 ... 60	0.02 ... 0.11	0.05 ... 0.09
No.3	0.06 ... 1.56	0.44 ... 4.44	0.12 ... 0.62	5 ... 73	0.09 ... 0.18	0.08 ... 0.12
Nebel						
No.4	0.50 ... 2.18	4.09 ... 6.98	0.51 ... 0.64	22 ... 60	0.04 ... 0.12	0.07 ... 0.07
No.5	0.47 ... 2.18	4.44 ... 6.56	0.51 ... 0.69	16 ... 69	0.03 ... 0.11	0.04 ... 0.06

Q = Discharge from interpolation of the flow velocities over the cross-sectional flow area.
A = Mean cross-sectional flow area.
r_{Hy} = Hydraulic Radius, ratio of A to the wetted perimeter.
Re = Reynolds-number, ratio of inertia induced forces to viscous forces.
Fr = Froude-number, ratio of mean velocity to wave propagation.
u^* = Shear velocity, $u^* \approx (g\ r_{Hy}\ I_E)^{0.5}$, with gravitational acceleration g and slope of energy I_E from surrounding water levels.

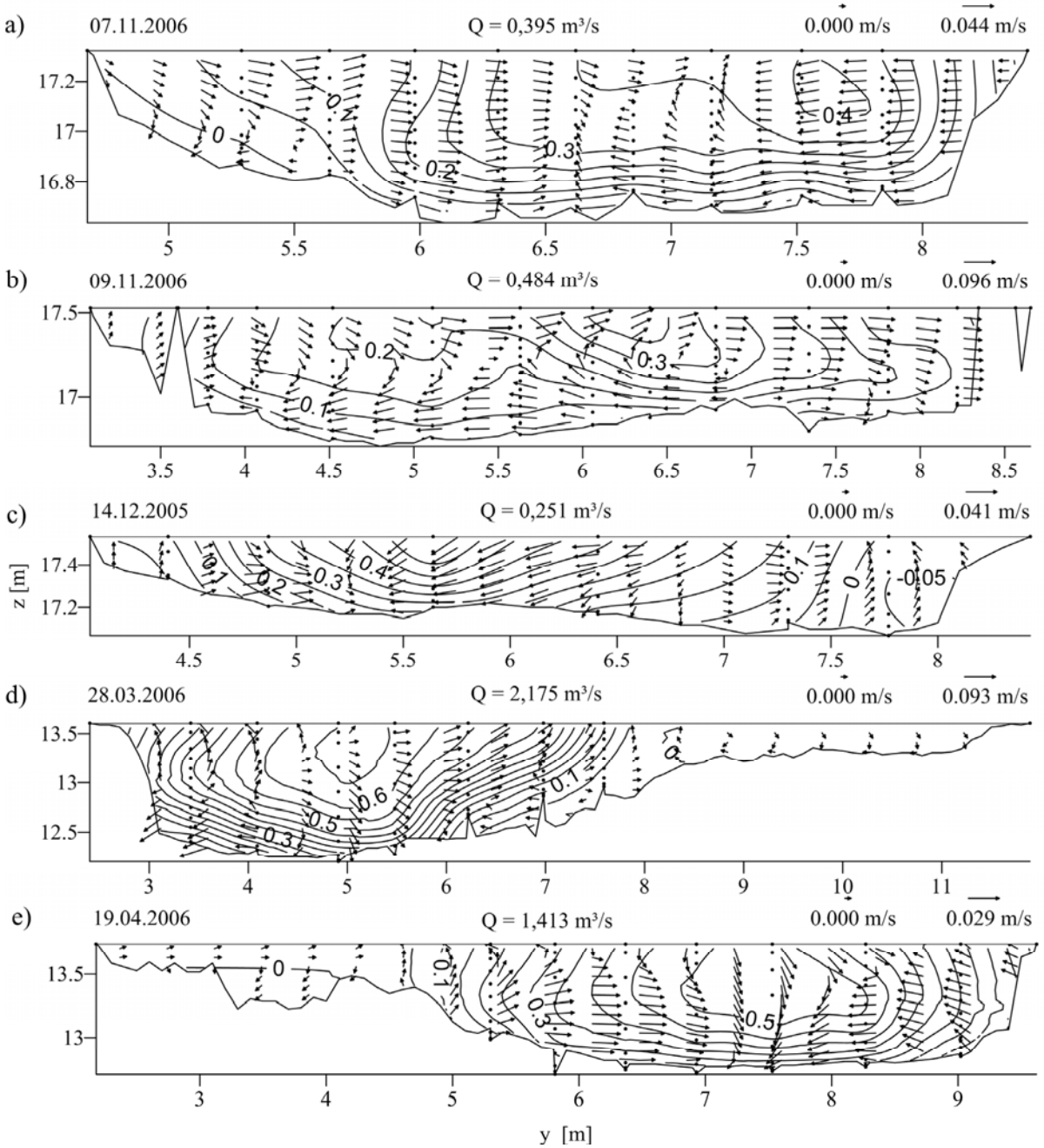

Figure 2. Examples of flow velocity and secondary currents at cross-sections a) No.1, b) No.2, c) No.3, d) No.4 and e) No.5 with the operative date, discharge rate and reference arrows above each plot. Isolines of the same flow velocities represent the distributions of 0.05 m/s steps. Arrows denote the secondary currents. Dots denote the ADV-sampling sites.

and secondary currents at the investigated cross-sections. These plots clearly reveal the non-uniform flow field in natural rivers. Lateral and vertical velocity gradients are of the same order of magnitudes suggesting a non-negligible bank roughness. Therefore velocity distributions were regarded in relation to the minimal distance ζ instead of the vertical distance z to the river bed (Fig.3). But even spatial averaged mean flow velocities with identical distances to the river bed were just weakly or not correlated to the logarithmic law of the wall obtained from least square fitting. The highest correlation coefficient was estimated once with $r < 0.9$ at cross-section No.4 and once with $r < 0.7$ at cross-section No.1. The plots of the secondary currents discover predominant converging (Fig.2a+e), circulating (Fig.2b), diverging (Fig.2d) or partly diverging and converging (Fig.2c) flow fields. These secondary currents were characteristic for the five cross-sections observed during every measurement and were caused by contracting or broadening river bed forms and by morphological structures upstream of the investigated cross-sections. In contrast, clear cellular or cylindrical inertia induced secondary currents were not detected. Even at the apex of a strong curvature (cross-section No.2), the present circular secondary currents (Fig.2b) rotated contrary to well known secondary currents of bankful meander flows (Kikkawa et al. 1976, Boxhall et al. 2003). Tab.2 contains the percentages of the secondary currents on the total veloc-

ity for the cross-sections. Ratios were higher at the restored river section (cross-section 1-3), but not negligible at both river sections.

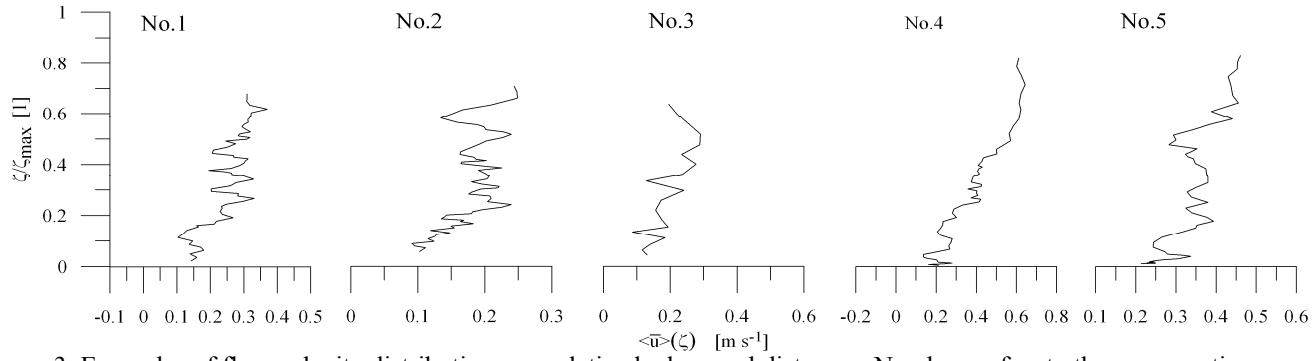

Figure 3. Examples of flow velocity distributions vs. relative bed normal distances. Numbers refers to the cross-sections.

Table 2. Ratios between secondary currents and total velocity

Cross-Sections No.	n	η [%]	σ [%]
1	8	17	5
2	6	51	13
3	5	37	14
4	8	9	2
5	7	15	2

n = number of measurements

$\eta = \langle (v^2+w^2)^{0.5}/(u^2+v^2+w^2)^{0.5} \rangle$; Note: < > denotes spatial, here geometrical mean values of all measurements at individual cross-sections.

σ = standard deviation of η

As a result, the whole flow field is three-dimensional and hence the momentum flux through turbulence as well as the momentum flux through secondary currents must be considered to total the momentum flux

$$d\dot{I} = d\dot{m} \cdot \vec{v} \tag{4}$$

where $d\dot{m}$ = mass flux and $\vec{v}$ = velocity vector. $d\dot{I}$ equals a force with the direction of $\vec{v}$ exerted on its surrounding area. The longitudinal component of the force relating to the parallel plane corresponds to the shear stress, which in respect to its temporal mean depends on the covariance between the longitudinal components u and its perpendicular component n of the velocity $\vec{v}$. The covariance of the vertical and lateral velocity fluctuations as well as the product of the mean vertical and lateral velocities do not cause any shear stress in longitudinally aligned layers, hence do not affect the longitudinal velocity distribution and are furthermore neglected. To total shear stress from fluctuating and mean velocities, one can simplify

$$\tau = \tau_{\overline{u'n'}} + \tau_{\overline{\overline{un}}} \tag{5}$$

where $\tau_{\overline{u'n'}}$ = turbulent, Reynolds shear stress, $\tau_{\overline{\overline{un}}}$ = shear stress from secondary currents. Note that n is the two-dimensional vector of v and w. The covariance between u and n can be estimated applying the mathematical rules to sum and multiply complex numbers. Therefore the velocity components can be described as complex numbers $u_r = u$, $u_i = 0$, $n_r = v$ and $n_i = w$ with the indices r for the real and i for the imaginary part. Hence, the time-averaged shear stress will be expressed through the magnitude $|\tau|$ and the angle φ of the principal shear stress

$$\tau = |\tau| \exp(i\varphi) \tag{6}$$

In contrast to dividing each component of the shear stress into two (Cartesian) parts, this transformation into a complex manner enables presenting the shear stress and its components in single plots, where the magnitude and the angle of the principal shear stress are directly observable. Fig.4 shows one example of the three terms of Eq.5, each estimated with Eq.6. It is obvious, that

Table 3. Mean shear stresses in the flow field, averaged about the cross-sectional areas and over all measurements, and mean river bed shear stress, averaged along 10...100 m sections (see text) and over all measurements at the cross-sections

Cross-Sec. No.	τ [N m-2]	$\tau_{\overline{u'n'}}$ [N m-2]	$\tau_{\overline{\overline{un}}}$ [N m-2]	$\tau_{\overline{u'n'}} / \tau_{\overline{\overline{un}}}$ [%]	τ_0 [N m-2]
No. 1	4.24	0.56	3.71	10	3.16
No. 2	6.38	1.02	5.74	16	5.27
No. 3	6.82	1.01	5.32	23	9.65
No. 4	6.81	0.69	6.43	12	4.87
No. 5	3.96	0.54	3.49	17	2.65

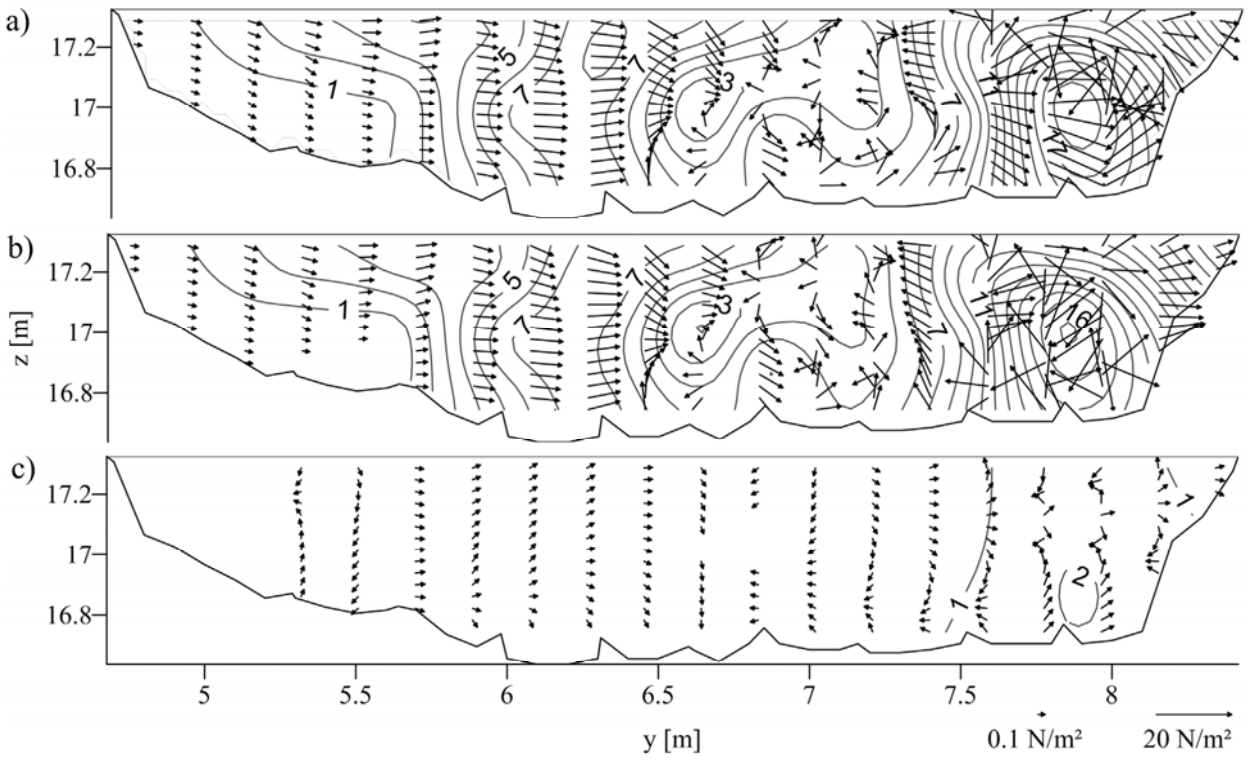

Figure 4. Example of a) total shear stress and shear stresses from b) secondary currents and c) turbulence at cross-section No.1 at the same operation date as the current profile in Fig.2a. The isolines and the arrow length denote value of the shear stress. Isolines of the same shear stress represent the distributions of 1 N m^{-2} steps. The angle of the principal shear stress φ is represented by the arrow alignment

the momentum fluxes were independent from the distances to the river bed. Tab.3 displays the geometric mean values of the shear stresses and the average ratio between the percentages of turbulence to secondary currents at the cross-sections. Therefore secondary currents always dominated the influence of turbulence and prevent the development of two-dimensional shear layers. The mean bed shear stress was estimated through

$$\tau_0 = \rho \cdot g \cdot r_{Hy} \cdot I_E \qquad (7)$$

where ρ = water density, g = gravity acceleration, r_{Hy} = hydraulic radius, which is the ratio between cross-sectional area and wetted perimeter and the energy slope I_E approximated by the ratio of water level difference along a 10...100 m longitudinal distance. At non-uniform flows it is not reasonable to estimate the bed shear stress by the local flow depth and the river bed slope. It must be noted, that τ_0 is the mean river bed shear stress of 10...100 m long river section, while τ, $\tau_{\overline{u'n'}}$ and $\tau_{\overline{un}}$ belong to particular cross-sections. Although the parameters represent different scales, resulting values are similar, especially for the comparison between the river bed shear stress and the shear stress caused by secondary currents. However, deviations up to one order of magnitude exist between the river bed shear stress and the Reynolds shear stress. Therefore, one may suggest that most of the shear stress and hence most of the flow resistance in natural river flows are caused by momentum fluxes through secondary currents.

4 DISCUSSION AND CONCLUSION

Field measurements in highly non-uniform rivers and creeks are posing a challenge. The necessary time for measurement is limited by the requirement of quasi-stationary time-spans or time-spans of daylight. Therefore, in comparison to laboratory studies, only few ADV-samples of relatively short record length have been used to analyse the flow and the momentum flux distributions and mean values. This circumstance may limit the accuracy of the hydraulic parameter and individual data, but do not change the general finding, that secondary currents resulting from mainly patchy morphological structures and river beds deliver the main contribution to the momentum flux. Vice versa Reynolds shear stresses, i.e., turbulent momentum fluxes are negligible for total momentum fluxes, independently from discharge rates at the cross-sections. As a result from all 34 cross-sectional measurements, recurrent pattern of momentum flux and velocity distribution were observed at the individual cross-sections, but without clear relationships to the river bed distances, as an essential characteristics of two-dimensional shear layers. In consequence, it is not suitable to

use models and equations of two-dimensional shear layer flows. Preceding data-processing, especially the realignment of velocity components in respect to the cross-sectional stream-line, is indispensible for analysing non-uniform flows. Otherwise, flow velocities will be under- and secondary currents will be overestimated. Actual investigations of open channel flows over different kinds of surface and form roughness used spatial averaged Reynolds-equations, i.e. double-averaged Navier-Stokes-equations to model flow and shear stress distributions (Nikora et al. 2007, Aberle et al. 2008). This concept could also be helpful to investigate particular or combinations of morphological structures in complex flow fields. Averaging should be performed simultaneously at different spatial scales within planes parallel to the river bed or to the morphological structures to estimate the hydraulic interaction of these structures. The present shear stresses from secondary currents correspond to the form-induced shear stress caused by structures of the scales up to the river bed within the respective cross-sectional plane.

REFERENCES

Aberle, J., K. Koll and A. Dittrich 2008. Form induced stresses over rough gravel-beds. Acta Geophysica (3) 56: 584-600.

Boxhall, J.B., I. Guymer and A. Marion 2003. Transverse mixing in sinuous natural open channel flows. Journal of Hydraulic Research (2) 41: 153-165.

Bradshaw, P. 1987. Turbulent Secondary Flows. Annual Review of Fluid Mechanics 19: 53-74.

Bravard, J.P. and F. Petit 2009. Geomorphology of Streams and Rivers. Encyclopedia of Inland Waters. E. L. Gene. Oxford: Academic Press. 387-395.

Buffin-Bélanger, T. and A.G. Roy 2005. 1 min in the life of a river: selecting the optimal record length for measurement of turbulence in fluvial boundary layers. Geomorphology 68: 77-94.

Carollo, F.G., V. Ferro and D. Termini 2002. Flow Velocity Measurements in Vegetated Channels. Journal of Hydraulic Engineering (7) 128: 664-673.

Falcón, M.A. and J.F. Kennedy 1983. Flow in alluvial-river curves. Journal of Fluid Mechanics 133: 1-16.

Goring, D.G. and V.I. Nikora 2002. Despiking Acoustic Doppler Velocimeter Data. Journal of Hydraulic Engineering (1) 128: 117-126.

Kikkawa, H., S. Ikeda and A. Kitagawa 1976. Flow and Bed Topography in Curved Open Channels. Journal of the Hydraulics Devision 102: 1327-1342.

Lesht, B.M. 1980. Benthic Boundary-Layer Velocity Profiles: Dependence on Averaging Period. Journal of Physical Oceanography 10: 985-991.

Lohrmann, A., R. Cabera and C.K. Nicholas (1994). Acoustic-Doppler Velocimeter (ADV) for laboratory use. Fundamentals and Advancements in Hydraulic Measurements and Experimentations: 351-365.

Manga, M. and J.W. Kirchner 2000. Stress partitioning in streams by large woody debris. Water Resources Research (8) 36: 2373-2379.

McLelland, S.J. and A.P. Nicholas 2000. A new method for evaluating errors in high-frquency ADV measurements. Hydrological Process (2) 14: 351-366.

Nezu, I. and H. Nakagawa 1993. Turbulence in Open-Channel Flows. Rotterdam: A.A. Balkema.

Nikora, V.I., S.R. McLean, S. Coleman, D. Pokrajac, I. McEwan, L. Campbell, J. Aberle, D. Clunie and K. Koll 2007. Double-Averaging Concept for Rough-Bed Open-Channel and Overland Flows: Applications. Journal of Hydraulic Engineering (8) 133: 884-895.

Rhoads, B.L. and A.N. Sukhodolov 2001. Field investigation of three-dimensional flow structure at stream confluences: 1. Thermal mixing and time-averaged velocities. Water Resources Research (9) 37: 2393-2410.

Sanjou, M., I. Nezu, T. Doi and H. Quang (2006). Coherent structure of horizontal eddies in meandering compound open-channel flow by using multi-layer scanning PIV. River Flow 2006. Lissabon: 243-252.

Stephan, U. and D. Gutknecht 2002. Hydraulic resistance of submerged flexible vegetation. Journal of Hydrology (1-2) 269: 27-43.

Sukhodolov, A., W.S.J. Uijttewaal and C. Engelhardt 2002. On the Correspondence between Morphological and Hydrodynamical Patterns of Groyne Fields. Earth Surface Processes and Landforms 27: 289-305.

Sukhodolov, A.N., H.P. Kozerski and B.L. Rhoads 2009. Currents in Rivers. Encyclopedia of Inland Waters. E. L. Gene. Oxford: Academic Press. 522-529.

Wang, X., Z. Wang, M. Yu and D. Li 2001. Velocity profile of sediment and comparison of log-law and wake-law. Journal of Hydraulic Research (2) 39: 211-217.